

negligible compared to the surface recombination velocity but the relative response comparing Figs. 1 and 3 is the same. Fig. 2 represents an intermediate case. These findings are in good qualitative agreement with the theoretical predictions of Gärtner's theory.

In order to explore the possibility of utilizing the PME spectral dependence as a tool for investigating changes in surface recombination velocity, a specimen was freshly etched and measured. A stream of air, saturated with HCl vapor was allowed to impinge on the illuminated surface of the sample. The results are shown in Fig. 4. It is noted that after treatment (curve 2) an inversion typical of increased front surface recombination velocity occurs, which after rinsing with water reverts to the original condition (curve 1).

It seems reasonable to expect that this effect could be utilized to study the effects of different environments on surface recombination velocities. If experimental conditions are established so that the PME response is at a null point and an environment is introduced which alters the surface recombination velocity, the PME effect could register either a positive or negative signal depending on whether the environment increased or decreased the recombination effect.

#### ACKNOWLEDGMENT

Acknowledgment is given to Dr. W. W. Gärtner for stimulating discussions on the interpretation of the experimental results obtained.

## Galvanomagnetic and Thermomagnetic Potentials in Zinc at Liquid Helium Temperatures\*

C. J. BERGERON, C. G. GRENIER, AND J. M. REYNOLDS

*Department of Physics, Louisiana State University, Baton Rouge, Louisiana*

(Received January 29, 1960; revised manuscript received April 21, 1960)

The Hall effect, magnetoresistance, thermoelectric voltage, and transverse Ettingshausen-Nernst potential have been measured in a single crystal of zinc in the liquid helium temperature range. Oscillations as a function of magnetic field strength were observed in all of these potentials. The measured period in  $1/H$  for the transverse oscillations was  $6.2 \times 10^{-5} \text{ gauss}^{-1} \pm 0.5\%$ , with the magnetic field parallel to the hexagonal axis. Both transverse effects possessed strong second harmonic oscillations. The oscillations in the longitudinal effects both exhibited a phase inversion in the neighborhood of 4.2 kgauss, the same field region for which the gross Hall field changed sign. In this same field region the period of the oscillations for the longitudinal effects was that of the second harmonic.

### I. INTRODUCTION

IN 1930 Schubnikow and de Haas<sup>1</sup> found that the transverse magnetoresistance of bismuth exhibited a magneto-oscillatory dependence at low temperatures. This led de Haas and van Alphen to their discovery of a similar behavior in the diamagnetic susceptibility of bismuth.<sup>2</sup> In recent years more attention has been given to the analogous oscillations in the galvanomagnetic and thermomagnetic effects in metals and semimetals such as Bi,<sup>3-11</sup> graphite,<sup>12-15</sup> Mg,<sup>16</sup> Sb,<sup>17</sup>

Empirical correlations between the reversal of sign of the Hall effect and: (1) the phase reversal of the magnetoresistance oscillations, (2) the strong second harmonic content of these oscillations in the region of the phase reversal, and (3) the quadratic shape of the envelope of the magnetoresistance oscillations in this region can be achieved by assuming the oscillatory component of  $\sigma_{21}$  to be much more significant than that of  $\sigma_{11}$ , where  $\sigma_{ik}$  is the conductivity tensor.

A further correlation between the oscillatory thermal effects can be achieved by assuming that the difference of the absolute thermoelectric power and the temperature derivative of the chemical potential is negligible.

Ga,<sup>18</sup> Sn,<sup>19,20</sup> Diamagnetic susceptibility oscillations in zinc were first observed by Marcus,<sup>21</sup> and later, the temperature dependence of the de Haas-van Alphen

<sup>6</sup> J. M. Reynolds, H. W. Hemstreet, T. E. Leinhardt, and D. D. Triantos, *Phys. Rev.* **96**, 1203 (1954).

<sup>7</sup> R. A. Connell and J. A. Marcus, *Phys. Rev.* **107**, 940 (1957).

<sup>8</sup> J. Babiskin, *Phys. Rev.* **107**, 981 (1957).

<sup>9</sup> S. Shalyt, *J. Phys. (U.S.S.R.)* **8**, 315 (1955).

<sup>10</sup> M. C. Steele and J. Babiskin, *Phys. Rev.* **94**, 1394 (1954).

<sup>11</sup> M. C. Steele and J. Babiskin, *Phys. Rev.* **98**, 359 (1955).

<sup>12</sup> D. Shoenberg, *Phil. Trans. Roy. Soc. (London)* **245**, 1 (1952).

<sup>13</sup> T. G. Berlincourt and M. C. Steele, *Phys. Rev.* **98**, 956 (1955).

<sup>14</sup> D. E. Soule, *Phys. Rev.* **112**, 698 (1958).

<sup>15</sup> D. E. Soule, *Phys. Rev.* **112**, 708 (1958).

<sup>16</sup> E. S. Borovik, doctoral thesis, Kharkov University, U.S.S.R., 1954 (unpublished).

<sup>17</sup> M. C. Steele, *Phys. Rev.* **99**, 1751 (1955).

<sup>18</sup> W. Yahia and J. A. Marcus, *Low-Temperature Physics and Chemistry*, edited by J. R. Dillinger (University of Wisconsin Press, Madison, 1958), p. 459.

<sup>19</sup> E. S. Borovik, *Doklady Akad. Nauk. S.S.S.R.* **69**, 767 (1949).

<sup>20</sup> P. B. Alers, *Phys. Rev.* **107**, 959 (1957).

<sup>21</sup> Jules A. Marcus, *Phys. Rev.* **71**, 559 (1947).

\* This work was supported by the Office of Ordnance Research, U. S. Army.

<sup>1</sup> L. Shubnikow and W. J. de Haas, *Leiden Comm. No. 207d* (1930).

<sup>2</sup> W. J. de Haas and P. M. van Alphen, *Leiden Comm. No. 212A* (1930).

<sup>3</sup> P. B. Alers and R. T. Webber, *Phys. Rev.* **91**, 1060 (1953).

<sup>4</sup> J. M. Reynolds, T. E. Leinhardt, and H. W. Hemstreet, *Phys. Rev.* **93**, 247 (1954).

<sup>5</sup> L. C. Brodie, *Phys. Rev.* **93**, 935 (1954).

parameters in zinc was studied by Berlincourt and Steele.<sup>22</sup> Borovik's<sup>23</sup> experiment on the transverse galvanomagnetic effects in zinc showed oscillations at very high fields. Alers<sup>24</sup> detected an oscillatory component in both the thermal and electrical magnetoresistance. This was confirmed in the work of Grenier et al.<sup>25</sup> who also reported oscillations in the Hall effect. It was reported at a later date that oscillatory thermomagnetic potentials were superimposed on the galvanomagnetic effects.<sup>26</sup> The oscillations in the Ettingshausen-Nernst effect and in the thermoelectric potentials were subsequently isolated, and preliminary measurements were done by Bergeron et al.<sup>27,28</sup>

The present study was undertaken as a first step toward an experimental determination of the components of a six by six tensor relating the electrical and thermal currents to the electric potentials and temperature gradients in a single zinc sample.

## II. NOTATION AND CONVENTION

Following the convention employed by Jan<sup>29</sup> in defining these effects:

$$E_i = \rho_{ik} J_k + \epsilon_{ik} G_k + (1/e) \partial E_0 / \partial x_i; \quad (1a)$$

and

$$w_i = -\pi_{ik} J_k + \lambda_{ik} G_k + (E_0/e) J_i, \quad (1b)$$

where  $\rho_{ik}$  = the electrical resistivity tensor,  $\lambda_{ik}$  = the thermal conductivity tensor,  $\epsilon_{ik}$  = the absolute thermoelectric power tensor,  $\pi_{ik}$  = the Peltier tensor,  $E_0$  = the chemical potential, the Fermi energy as measured from the nearest zone boundary,  $e$  = the electronic charge (negative number),  $w_i$  = the heat current density of carriers,  $J_k$  = the electric current density,  $E_i$  = the electric field,  $G_k$  = the negative gradient of the absolute temperature, and  $i, k = 1, 2, 3$ . All of the various tensors have an arbitrary magnetic field dependence. However, it will be convenient to distinguish between the purely oscillatory effects of these tensors and their gross or smoothly varying field dependence, e.g.,  $\rho_{ik} = \bar{\rho}_{ik} + \tilde{\rho}_{ik}$ , where  $\bar{\rho}_{ik}$  expresses the nonoscillatory field dependence and  $\tilde{\rho}_{ik}$  the oscillatory component.

It can be seen from Eqs. (1a) and (1b) that the isothermal Hall effect and magnetoresistance are characterized by  $\rho_{21}$  and  $\rho_{11}$ , respectively; and the isothermal Ettingshausen-Nernst effect and absolute

thermoelectric power by  $\epsilon_{21}$  and  $\epsilon_{11}$ . With reference to Fig. 1(a) the distinction between the adiabatic and the isothermal case is the following:

$$w_2 = 0; \text{ adiabatic,} \quad (2a)$$

$$G_2 = 0; \text{ isothermal.} \quad (2b)$$

Although Eqs. (1a) and (1b) were defined in terms of an isotropic medium, they can be applied to a crystallographic system if there is sufficient symmetry between the system and the field and current vectors. With reference to Fig. 1(b), if the magnetic field is in the  $z$  direction, it is not necessary that the medium be strictly isotropic, but only that there be isotropy in the  $x$ - $y$  plane.<sup>30</sup> This is guaranteed by Onsager's reciprocal relations if a crystalline axis of three-, four-, or sixfold symmetry lies along the  $z$  direction.<sup>31</sup>

Since the theorist calculates the components of the conductivity tensor and then performs a matrix inversion to arrive at explicit expressions for the magnetoresistance and Hall coefficient, it is only under special conditions that the expressions for these quantities are amenable to comparison with experimental data. Therefore, it is in general more profitable to reverse this procedure and to transform the experimental

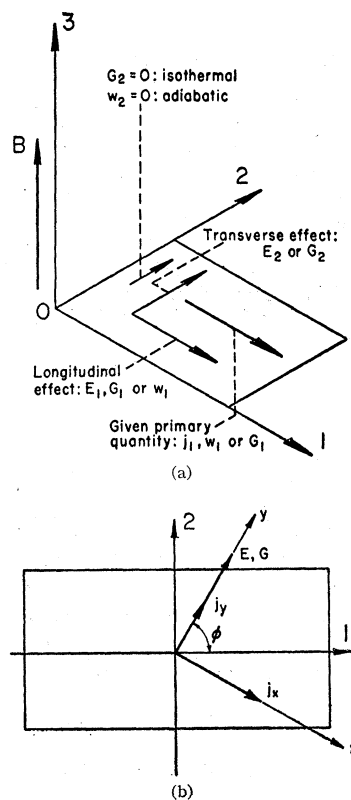


FIG. 1. A schematic representation of the field and current quantities in a flat rectangular sample.

<sup>22</sup> T. G. Berlincourt and M. C. Steele, Phys. Rev. **95**, 1421 (1954).

<sup>23</sup> E. S. Borovik, J. Exptl. Theoret. Phys. (U.S.S.R.) **30**, 262 (1956) [translation: Soviet Phys.—JETP **3**, 243 (1956)].

<sup>24</sup> P. B. Alers, Phys. Rev. **101**, 41 (1956).

<sup>25</sup> C. G. Grenier, J. M. Reynolds, and S. A. Ali, *Low-Temperature Physics and Chemistry*, edited by J. R. Dillinger (University of Wisconsin Press, Madison, 1958), p. 457.

<sup>26</sup> C. G. Grenier, C. J. Bergeron, and J. M. Reynolds, Bull. Am. Phys. Soc. **4**, 6 (1959).

<sup>27</sup> C. J. Bergeron, C. G. Grenier, and J. M. Reynolds, Bull. Am. Phys. Soc. **4**, 5 (1959).

<sup>28</sup> C. J. Bergeron, C. G. Grenier, and J. M. Reynolds, Phys. Rev. Letters **2**, 40 (1959).

<sup>29</sup> J. P. Jan, in *Solid-State Physics*, edited by F. Seitz and D. Turnbull (Academic Press, Inc., New York, 1957), Vol. 5.

<sup>30</sup> H. B. Callen, Phys. Rev. **73**, 1349 (1948).

<sup>31</sup> L. Onsager, Phys. Rev. **37**, 405 (1931); **38**, 2265 (1931).

Hall effect and magnetoresistance data into the various components of the conductivity tensor. For a two-dimensional isotropic case,

$$\sigma_{21} = \rho_{21}/(\rho_{21}^2 + \rho_{11}^2); \quad \sigma_{11} = \rho_{11}/(\rho_{21}^2 + \rho_{11}^2). \quad (3)$$

Since the thermomagnetic effects were measured with a constant heat current,  $w_1$  [see Fig. 1(a)], and not with a constant temperature gradient,  $G_1$ , and also under adiabatic conditions, the experimental data were not a direct measure of  $\epsilon_{21}$  and  $\epsilon_{11}$ , rather of  $\epsilon_{11}'$  and  $\epsilon_{21}'$ , where

$$\epsilon_{11}' = E_1/w_1 = \{[\epsilon_{11} - (1/e)\partial E_0/\partial T] - \epsilon_{21} \tan \varphi'\} \lambda_{11}^{-1}, \quad (4a)$$

$$\epsilon_{21}' = E_2/w_1 = \{\epsilon_{21} + [\epsilon_{11} - (1/e)\partial E_0/\partial T] \tan \varphi'\} \lambda_{11}^{-1}. \quad (4b)$$

$\lambda_{11}^{-1}$  is the diagonal component of the thermal magnetoresistance tensor, and  $\varphi'$  is the Righi-Leduc angle.

$$\lambda_{11}^{-1} = \lambda_{11}/(\lambda_{11}^2 + \lambda_{21}^2); \quad \tan \varphi' = G_2/G_1. \quad (5)$$

### III. THEORY

Most of the theories of galvanomagnetic and thermomagnetic phenomena are classical treatments. Hence, the oscillatory behavior observed at low temperatures is unexplained by these theories since the origin of these oscillations is essentially quantum mechanical. However, in recent years calculations by Lifshitz and Kosevich,<sup>32</sup> and Zil'berman<sup>33</sup> have taken into account the effect of the orbital quantization (due to an applied magnetic field) upon the galvanomagnetic and thermomagnetic properties.

Zil'berman's approach is the more standard of the two. A two-band model with a field independent relaxation time and an isotropic quadratic dispersion law is assumed. Introducing lattice defects as a perturbation to a perfect-lattice Hamiltonian, which already includes the electric and magnetic fields, the component of the magnetoconductivity tensor in the direction of the electric field,  $\sigma_{11}$  is calculated:

$$\sigma_{11} = (e/H^2)f, \quad (6)$$

where

$$f = (8/3)m^4A[1 - (9/40)\beta H/E_0 - 5\pi^2\sqrt{2}kT/(\beta HE_0)^{3/2}e^{-\gamma} \cos(\eta - \pi/4) + \dots].$$

In the above expression for  $f$ ,  $\gamma = 2\pi^2kT/\beta H$ , and  $\eta = 2\pi E_0/\beta H$ . The symbols,  $k$ ,  $T$ , and  $\beta$ , are the Boltzmann constant, the absolute temperature, and the double effective Bohr magneton, respectively.  $A$  is a constant which is directly proportional to the lattice defect concentration. For the case of two overlapping conduction bands,  $\sigma_{11} = (e/H^2)(f_1 + f_2)$  with subscripts

"1" and "2" applied to  $m$ ,  $\beta$ , and  $\eta$  for  $f_1$  and  $f_2$ , respectively, and  $E_0$  is replaced by  $(A_0 - E_0)$  for  $f_2$ .  $A_0$  is the overlap of the upper and lower bands.

The perturbation of the lattice defects is neglected in deriving the expression for  $\sigma_{21}$ , and the result is identical to the case of particles in a box for crossed electric and magnetic fields:

$$\sigma_{21} = ec(N_1 - N_2)/H, \quad (7)$$

where  $N_1$  and  $N_2$  are the numbers of electrons and holes, respectively.

In their analysis of the electrical conductivity Lifshitz and Kosevich<sup>32</sup> relate the oscillations in the components of the conductivity tensor to the oscillations in the diamagnetic susceptibility. These authors find that the oscillatory terms in the conductivity tensor are proportional to the product of the classical mobility tensor and the oscillatory term of the magnetization. However, the components of the mobility tensor are evaluated only under the same simplifying, and hence, limiting assumptions employed by Zil'berman, e.g., elastic isotropic scattering, etc.

The expression for the fundamental period,  $P$ , for one band is related to the extremum cross sectional area of the Fermi surface,  $A_m$ , perpendicular to the applied magnetic field:

$$P = eh/cA_m, \quad (8)$$

where  $A_m$  is in momentum units. This is the Onsager-Lifshitz relation.<sup>34-36</sup>

As can be seen from Eq. (6), the period is also given by,

$$P = \beta/E_0. \quad (9)$$

The conditions on the temperature, the magnetic field, and the electronic parameters of the material that are generally invoked in the contemporary theories of these effects are:

$$\begin{aligned} (a) \quad kT/\beta H < 1, \\ (b) \quad kT/E_0 \ll 1, \\ (c) \quad \beta H/E_0 \ll 1. \end{aligned} \quad (10)$$

Condition (a) assumes Fermi surfaces which are sharp compared to the energy difference between successive orbital levels. Condition (b) requires that the de Haas-van Alphen type carriers obey Fermi-Dirac statistics. The physical implication of condition (c) is that the number of orbital levels below the Fermi surface is large. Generally, this is required for purposes of calculational expediency in the evaluation of partial sums over the number of levels. If this number is sufficiently large, these sums can be approximated by

<sup>34</sup> L. Onsager, *Phil. Mag.* **43**, 1006 (1952).

<sup>35</sup> I. M. Lifshitz, reported to a meeting of the Ukrainian Academy of Science, U.S.S.R., in January, 1951 (unpublished).

<sup>32</sup> I. M. Lifshitz and L. M. Kosevich, *J. Exptl. Theoret. Phys. (U.S.S.R.)* **33**, 88 (1957) [translation: *Soviet Phys.—JETP* **6**, 67 (1958)].

<sup>33</sup> G. E. Zil'berman, *J. Exptl. Theoret. Phys. (U.S.S.R.)* **29**, 762 (1955) [translation: *Soviet Phys.—JETP* **2**, 650 (1956)].

<sup>36</sup> I. M. Lifshitz, M. Ia. Azbel, and M. I. Kaganov, *J. Exptl. Theoret. Phys. (U.S.S.R.)* **31**, 63 (1956) [translation: *Soviet Phys.—JETP* **4**, 41 (1957)].

Poisson integrals. These are in turn evaluated by means of Fresnel integrals at infinite limits, which is another approximation that requires the applicability of condition (c) for validity.<sup>33,37,38</sup> However, in the present investigation this last condition is the one most open to question.

Zil'berman has also calculated a relationship between the electric field and the temperature gradient in the direction of the electric field, the  $y$  direction of Fig. 1(b).

$$E_y^* = \frac{2}{3}(g/eE_0)G_y,$$

where  $E^*$  is the negative gradient of the electrochemical potential.

$$E_y^* = E_y + (1/e)\partial E_0/\partial y,$$

and

$$g = 1 - \frac{9\beta H}{80E_0} + \frac{15}{2\pi\sqrt{2}} \frac{(\beta HE_0)^{\frac{1}{2}}}{kT} e^{-\gamma} (1-\gamma) \sin(\eta - \pi/4).$$

The expression for  $g$  is for a single band. The two-band model generates a more complex expression of the same form.

It is interesting to note that in the thermal case Zil'berman's theory gives no appreciable monotonic component. Also, the explicit dependence on the imperfections of the lattice is lost. However, this can probably be restored, implicitly at least, through the introduction of a Dingle<sup>39</sup> damping factor  $\exp(-2\pi^2 kx/\beta H)$ , ( $x = \hbar/2\pi^2 k\tau$ , and  $\tau$  is the relaxation time of the carriers) into the amplitude of the oscillatory terms. A similar damping factor could also be introduced into the oscillatory terms of the components of the electrical conductivity tensor, Eqs. (6) and (7).

This calculation is incomplete in the sense that it ignores the possible existence of a temperature gradient in the  $x$  direction. For a single-band model, this theory gives the following thermoelectric tensor components:

$$\epsilon_{11} = \frac{2}{3}g/eE_0, \quad (11a)$$

$$\epsilon_{21} = 0 \text{ (or negligible)}. \quad (11b)$$

Following a phenomenological calculation by Azbel et al.<sup>40</sup> of galvanomagnetic and thermomagnetic effects, it is demonstrated that the Wiedemann-Franz ratio holds for all components of the electrical and thermal conductivity tensors at very low temperatures for a magnetic field of arbitrary magnitude and direction. The salient point of this calculation is a demonstration of the equality of the relaxation times for electrical and thermal transport processes under various extreme physical conditions.

<sup>37</sup> M. Blackman, Proc. Roy. Soc. (London) **A166**, 1 (1938).

<sup>38</sup> J. S. Lvinger and E. G. Grimsal, Phys. Rev. **94**, 772(A) (1954); and E. G. Grimsal, thesis, Louisiana State University, 1954 (unpublished).

<sup>39</sup> R. B. Dingle, Proc. Roy. Soc. (London) **A211**, 500 (1952).

<sup>40</sup> M. Ia. Azbel, M. I. Kaganov, and I. M. Lifshitz, J. Exptl. Theoret. Phys. (U.S.S.R.) **32**, 1188 (1957) [translation: Soviet Phys.—JETP **5**, 967 (1957)].

The implication of the validity of the Wiedemann-Franz ratio is that the Hall and Righi-Leduc angles are identical. Therefore, in Eqs. (4a) and (4b) which give the experimental  $\epsilon'$  tensor components, the experimentally determined Hall angle can be substituted for the Righi-Leduc angle. Applying this to Eqs. (4a), (4b), and (11b),

$$\epsilon_{21}' = \epsilon_{11}' \tan \varphi. \quad (12)$$

#### IV. EXPERIMENTAL

All data were taken with the magnetic field directed along the hexagonal axis, thus satisfying the necessary symmetry conditions for two-dimensional isotropy. The electrical or heat current through the crystal was held at a constant value. The electrical current was 1 ampere  $\pm 0.1$  ampere. During any given field sweep, the current was constant to within less than 1%; but, a 10% variation from one set of experiments to the next was possible depending on the state of charge of the current batteries. However, all electrical data were normalized to a current of 1 ampere and to a standard amplification of 10-cm recorder deflection per 100 millimicrovolts. The heat current was of the order of 4 milliwatts.

The electromagnet used in these experiments was an iron core Weiss magnet with 8-inch pole pieces separated by a  $1\frac{5}{8}$ -inch air gap. It could be rotated  $360^\circ$  about a vertical axis. Any angular position of the magnet could be reproduced to within one-fourth of a degree. The magnet was calibrated by a nuclear resonance flux meter. As Alers<sup>24</sup> has pointed out, there exists a sharp relative minimum in the magneto-resistance of a zinc crystal when the magnetic field is directed along the hexagonal axis. Thus, the magnetic field was easily oriented along the hexagonal axis at the beginning of each experiment.

A "thermal-free" microvolt potentiometer was used as a bias voltage source in performing these potential measurements. The potentials were amplified by a dc 8-cps breaker amplifier and recorded by a Brown recorder. With suitable choice of electrical shielding, placing of measuring equipment, etc., it was possible to discriminate voltages of the order of a millimicrovolt over a range of 10 microvolts. A continuous signal was achieved by increasing the magnet current at a constant rate. Thus, in the region of the magnetic field where the field is directly proportional to the current (up to 10 kgauss) the trace of the signal on the Brown recorder was linearly related to the magnetic field. Whenever the magnet current increased by a prescribed amount, a pip was superimposed on the Brown recorder trace. The linearity of the magnetic field was also used to isolate the oscillatory component of the magnetoresistance  $\tilde{\rho}_{11}$  and to display it directly as a Brown recorder trace. A voltage divider network across the magnet was used to produce an increasing potential as a function of magnetic field strength. This potential was introduced

as a "bucking" voltage in opposition to the output of the dc amplifier when a measurement was being made of the magnetoresistance. Thus, the Brown recorder traced a curve in which the oscillatory component of the magnetoresistance could appear clearly, as most of the large monotonic part was compensated.

The sample was chemically cut from a single crystal of zinc grown by a modified Bridgman method. The sample dimensions were  $26.58 \times 8.1 \times 0.345$  mm. It was cut from the mother crystal in such a manner that when placed vertically in the cryostat (i.e., the long length of the crystal being vertical) its hexagonal axis lay in the horizontal plane making an angle of  $44^\circ$  with the normal to the large face of the crystal. Its orientation was carefully determined by an x-ray diffraction study.

For the galvanomagnetic experiments the crystal lay on the flat bed of the Lucite holder, Fig. 2, and was held in place by work-hardened copper pressure contacts. Originally both potential and current leads were connected in this manner to the sample; however, it was noted that the contact resistance caused a production of heat at the current probes and a net heat flow through the crystal.<sup>41</sup> Later the current leads were soldered directly to the ends of the crystal to isolate the galvanomagnetic potentials. After the Hall leads had been soldered to the pressure contacts, they were brought directly together along the line defined by the Hall contacts. They were then twisted together so as to minimize the areal projection of the loop formed by the leads, the pressure contacts, and the crystal when viewed from above. This was a successful procedure

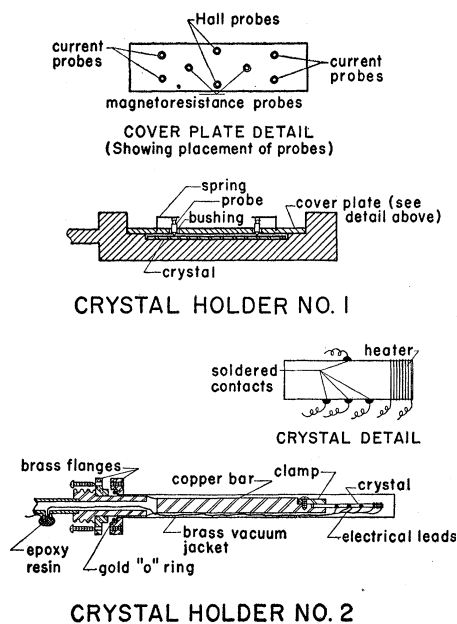


Fig. 2. The crystal holders for the galvanomagnetic (number 1) and thermomagnetic (number 2) effects.

<sup>41</sup> This spurious heat current originally brought to our attention the thermomagnetic potentials.

since the emf induced in the transverse leads by the constantly increasing magnetic field was negligible.

In most of the experiments the magnetic field was directed along the hexagonal axis, i.e., at an angle of  $44^\circ$  to the normal of the crystal; hence, there was no feasible way in which the same procedure could be applied to the magnetoresistance leads. Therefore, a compensating loop was introduced into the longitudinal leads themselves about a centimeter above the upper edge of the crystal. The orientation of this second loop was such that the emf induced in it by the increasing magnetic field opposed the emf induced in the crystal loop. To achieve sufficiently good compensation, a trial and error process of adjusting the area of the compensating loop was necessary.

The calorimeter-crystal holder used for measuring the thermomagnetic potentials is shown in Fig. 2. The sample was clamped to the copper bar extending down into the brass vacuum jacket. It was insulated electrically from the bar by means of cigarette paper impregnated with silicone vacuum grease. Around its lower end was wrapped a 40-gauge resistance wire heater. The longitudinal and transverse potential leads were soldered directly to the crystal and were brought from the vacuum system into the helium bath through an epoxy resin seal.<sup>42</sup> The emf's induced in the potential leads-crystal loop were compensated for in the same manner as in the galvanomagnetic case. The same measuring apparatus that was used in the galvanomagnetic experiments was employed in the thermal measurements.

The galvanomagnetic potentials were measured under isothermal conditions so that  $G_1 = G_2 = G_3 = 0$  and with the current flowing in the 1 direction  $J_2 = J_3 = 0$ .

The field tensor reduces to

$$E_1 = \rho_{11}J_1, \quad E_2 = \rho_{21}J_1, \quad E_3 = \rho_{31}J_1.$$

If  $\mathbf{d}$  is the vector distance between the probes, the measured potential is given by

$$V = -\mathbf{d} \cdot \mathbf{E} = -J_1(\rho_{11}d_1 + \rho_{21}d_2 + \rho_{31}d_3),$$

where  $d_1$ ,  $d_2$ ,  $d_3$  are components of the probe distance along the current, mutually perpendicular to the current and the field, and parallel to the field, respectively.

In the Hall effect measurements the misalignment of the probes,  $d_1$ , introduces a magnetoresistance effect. The effective probe separation for the Hall effect is  $d_2$ , and  $d_3$  is the probe separation along the magnetic field direction. In this case where the hexagonal axis is parallel to the field, but makes an angle  $\theta$  with the normal to the large face of the crystal:

$$d_2 = d \cos\theta, \quad d_3 = d \sin\theta.$$

$$V_1 = -J_1\rho_{11}d_1 \quad \text{and} \quad V_1(H) = V_1(-H).$$

$$V_2 = -J_1\rho_{21}d_2 \quad \text{and} \quad V_2(H) = -V_2(-H).$$

$$V_3 = -J_1\rho_{31}d_3 \quad \text{and} \quad V_3(H) = V_3(-H), \quad \text{or} \quad 0.$$

<sup>42</sup> K. S. Balain and C. J. Bergeron, Rev. Sci. Instr. 30, 1058 (1959).

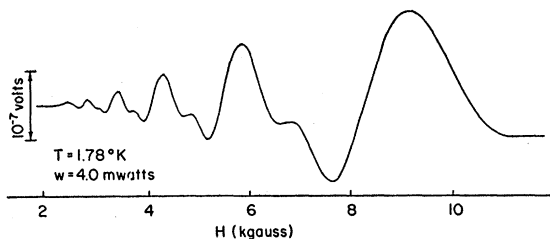


FIG. 3. The potential from which  $\epsilon_{21}'$  is computed.

$V_3=0$  when  $H$  is in the hexagonal direction and the current is perpendicular to it. In case of misalignment of the field with the hexagonal axis  $V_3(H) = V_3(-H)$ .<sup>23</sup> Therefore,  $V(H) - V(-H) = 2V_2(H)$  and

$$\rho_{21} = -[V(H) - V(-H)]/2J_1d \cos\theta.$$

Measurements were made for both  $H$  and  $-H$  and  $\rho_{21}$  was deduced from the above equation. The magnetoresistance probe misalignment was negligible, and a single sweep of the field,  $H$ , was sufficient in this case.

Similar arguments also hold for the thermomagnetic potentials measured under the conditions:

$$J_1 = J_2 = J_3 = 0, \quad w_2 = w_3 = 0,$$

with  $E_1 = \epsilon_{11}'w_1$ ,  $E_2 = \epsilon_{21}'w_1$ ,  $E_3 = \epsilon_{31}'w_1$ , and

$$V = -(\epsilon_{11}'d_1 + \epsilon_{21}'d_2 + \epsilon_{31}'d_3)w_1.$$

Therefore,  $\epsilon_{21}' = [V(-H) - V(H)]/2w_1d \cos\theta$ . The quantity,  $\epsilon_{21}'$ , was obtained by measuring the voltage across the sample using the Hall probes.

Early experiments were performed employing reversal of the field, but the potentials due to  $\epsilon_{11}'$  and  $\epsilon_{31}'$  turned out to be negligible and a single sweep of  $H$  was sufficient for the determination of  $\epsilon_{21}'$ . Using the magnetoresistance probes,  $\epsilon_{11}'$  could be measured. No reversal of the field was needed.

In the measurement of the Ettingshausen-Nernst and thermoelectric voltage, since the conditions were not isothermal, a temperature difference existed between the potential measuring probes. In most of these experiments the probes were hard-worked copper. In principle, a correction should be made to take account of the Cu-Zn thermocouple emf generated at the probes. For example, due to the Righi-Leduc effect, a temperature difference will appear between the probes during an Ettingshausen-Nernst measurement in such a way that a thermocouple emf proportional to the

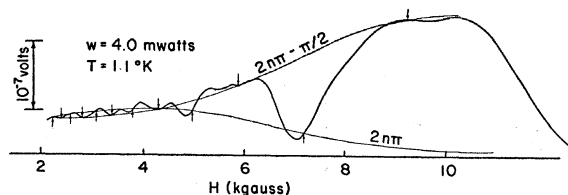


FIG. 4. The potential from which  $\epsilon_{11}'$  is computed.

Righi-Leduc effect will be superimposed on the Ettingshausen-Nernst voltage. In fact, this effect, analogous to the Hall effect, should have a reversal of sign around 4.5 kgauss. No effect having such behavior could be detected in the Ettingshausen-Nernst measurements. Thus, no correction for the Cu-Zn thermocouple emf was attempted.

## V. RESULTS

The trace of the Brown recorder gave a continuous record of the field variation of the various potentials. Some of these curves are reproduced in Figs. 3, 4, and 5. The transverse and longitudinal thermomagnetic potentials are represented in Figs. 3 and 4, respectively, and the compensated magnetoresistance trace is seen in Fig. 5. The period for the Hall effect oscillations, i.e.,

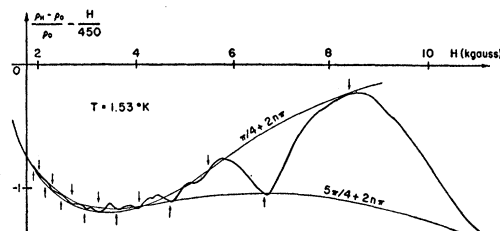


FIG. 5. The compensated magnetoresistance potential.

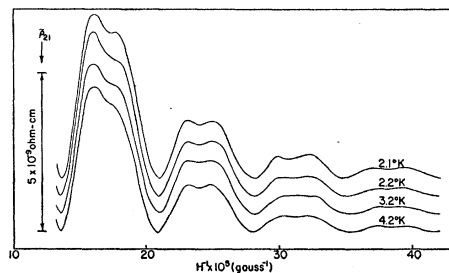


FIG. 6. The oscillatory component of the Hall effect  $\bar{\rho}_{21}$ , for various temperatures.

the oscillations of  $\bar{\rho}_{21}$ , Fig. 6, is  $6.14 \times 10^{-5}$  gauss<sup>-1</sup>, and for  $\epsilon_{21}'$ , Fig. 7, it is  $6.22 \times 10^{-5}$  gauss<sup>-1</sup>. The phase angle for  $\bar{\rho}_{21}$  for a cosine dependence is  $0 \pm 0.03\pi$  and is  $\pi/2 \pm 0.02\pi$  for  $\epsilon_{21}'$ . The average period of  $\bar{\rho}_{11}$  and  $\epsilon_{11}'$  in the low and high field regions of the oscillations is  $\sim 6.3 \times 10^{-5}$  gauss<sup>-1</sup>. These results are also given in Table I along with similar results for other transport and magnetic oscillatory phenomena in zinc.

The oscillations in the Hall and Ettingshausen-Nernst effects, Figs. 8 and 9, possess the same double peak system, although the second peak is less pronounced in  $\bar{\rho}_{21}$ . This is in part caused by the graphical method of calculating  $\bar{\rho}_{21}$ , i.e., a smooth envelope curve,  $\bar{\rho}_{21}$ , is drawn tangent to peaks in  $\rho_{21}$ , Fig. 7.  $\bar{\rho}_{21}$  is then defined as  $(\rho_{21} - \bar{\rho}_{21})$ . The cusp-like appearance of the maxima and minima in  $\epsilon_{21}'$  has been observed in other materials such as graphite<sup>15</sup> and bismuth.<sup>8</sup> A qualitative

discussion of this phenomenon and its interpretation has been given by Babiskin.<sup>8</sup>

There is a great deal of similarity between the oscillatory components of the magnetoresistance (see Fig. 10) and the thermoelectric potential. As shown in Figs. 4 and 5, they both exhibit a phase inversion in the amplitude of their oscillations between 4 and 5 kgauss. This phase inversion is illustrated in the following way: An average period,  $P$ , is chosen ( $6.3 \times 10^{-5}$  gauss<sup>-1</sup> for both  $\epsilon_{11}'$  and  $\tilde{\rho}_{11}$ ). A phase angle  $\alpha$  is then chosen ( $\alpha = \pi/4$  for  $\tilde{\rho}_{11}$ ;  $\alpha = -\pi/2$  for  $\epsilon_{11}'$ ) that will cause  $P(n + \alpha/2\pi)$  to give a value of magnetic field corresponding to the maximum in the neighborhood of 9 kgauss ( $n = 1, 2, 3, \dots$ ). This is indicated by the first arrow in the upper curve starting from the right. To calculate the field value for the next equiphase

TABLE I. Periods and phases of oscillatory effects in zinc along the hexagonal axis.

Effect	Period $\times 10^5$ gauss <sup>-1</sup>	Phase <sup>a</sup>
$\rho_{11}^b$	6.3 (above and below phase inversion point)	
$\rho_{11}^c$	5.3	
$\rho_{11}^e$ (another sample)	5.8	
$\rho_{21}^b$	6.14	0
$\epsilon_{21}'^b$	6.22	$+\pi/2$
$\epsilon_{11}'^b$	6.3 (above and below phase inversion point)	
$\lambda_{11}^{-1} e$	6.0	0
$\Delta\chi^d$	6.4	$-\pi/4$
$\Delta\chi^e$	5.3	
$\Delta\chi^e$ (another sample)	6.05	
$\Delta\chi^f$	6.4	$-\pi/4$
$\Delta\chi^g$	6.3	$+\pi/4$

<sup>a</sup> For a cosine dependence.  
<sup>b</sup> Present study.  
<sup>c</sup> P. B. Alers, Phys. Rev. **101**, 41 (1956).  
<sup>d</sup> T. G. Berlincourt and M. C. Steele, Phys. Rev. **95**, 1421 (1954).  
<sup>e</sup> I. M. Dmitrenko, B. I. Verkin, and B. G. Lazarev, J. Exptl. Theoret. Phys. (U.S.S.R.) **35**, 328 (1958) [translation: Soviet Phys. —JETP **8**, 229 (1959)].  
<sup>f</sup> J. S. Dhillon and D. Schoenberg, Phil. Trans. Roy. Soc. (London) **A248**, 1 (1955).  
<sup>g</sup> B. I. Verkin and I. M. Dmitrenko, Izvest. Akad. Nauk S.S.S.R. **19**, 409 (1955).

point  $6.3 \times 10^{-5}$  gauss<sup>-1</sup> is added to the reciprocal field value of the first point. This field value is indicated by the second arrow from the right on the top curve. This process is repeated in order to calculate successive phase points for the top curve. It is then noted that these equiphase points, although initially occurring at or near maxima, become progressively coincident with minima at lower field values. By the same procedure another set of equiphase points is calculated, but these points are a plus one-half period out of phase with the first set of points. The intersection of the upper and lower smooth curves drawn through equiphase points indicates the neighborhood of the phase reversal. As has already been noted, this occurs at about 4.3 kgauss for both oscillations, which is the same neighborhood of magnetic field at which  $\rho_{21}$  reverses sign, as shown in Fig. 8. An empirical correlation between the reversal

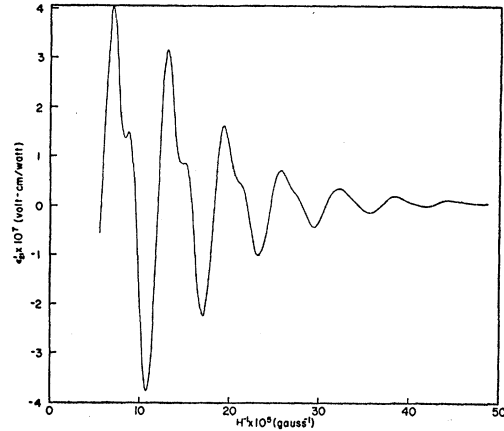


FIG. 7. The effective Ettingshausen-Nernst potential,  $\epsilon_{21}'$ , versus the reciprocal of the magnetic field.

of sign of  $\rho_{21}$  to the reversal of phase of  $\tilde{\rho}_{11}$  will be developed in the discussion.

The periods of the thermoelectric potential and magnetoresistance are not uniform. This is especially true in the neighborhood of the phase inversion where the second harmonic is dominant to the extent that the effective period is half its high and low field value. This can be seen clearly in the plot of the thermoelectric potential vs  $1/H$ , Fig. 9. There was an apparent phase difference of  $3\pi/4$  between these two effects, although it is of dubious value to talk of a phase relation for these two quantities since their apparent period is not a constant.

VI. DISCUSSION

Magnetoresistance Tensor

The reversal of sign of the Hall effect in zinc has also been observed by Borovik.<sup>23</sup> Similar anomalies in the low magnetic field region have been reported in the Hall effect in aluminum<sup>43</sup> and graphite.<sup>14</sup> Borovik<sup>43</sup> fitted the

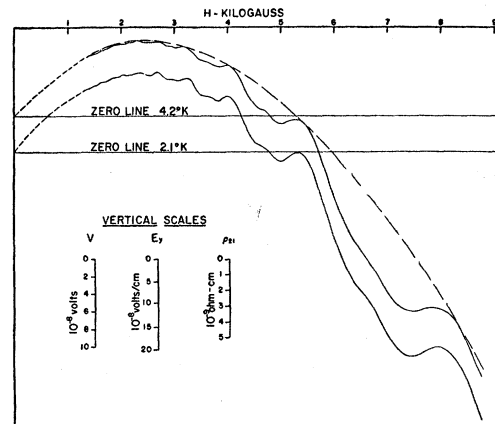


FIG. 8. The total Hall effect,  $\rho_{21}$ , versus the magnetic field,  $H$ .

<sup>43</sup> E. S. Borovik, Doklady Akad. Nauk S.S.S.R. **70**, 601 (1950); and J. Exptl. Theoret. Phys. (U.S.S.R.) **23**, 83 (1953).

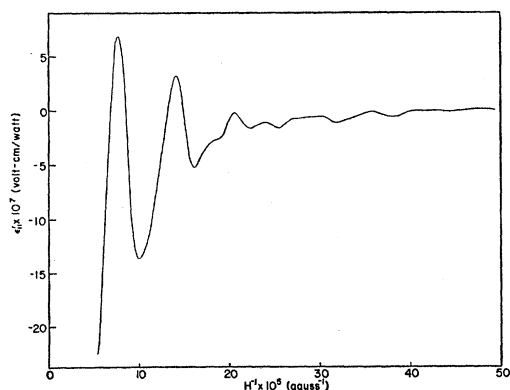


FIG. 9. The effective thermoelectric power,  $\epsilon_{11}'$ , versus the reciprocal of the magnetic field.

data for aluminum to a Sondheimer-Wilson type theory<sup>44</sup> by introducing an additional pair of electron and hole carriers, thereby creating a sufficient number of parameters to produce an empirical fit. Soule<sup>44</sup> used essentially the same procedure in his analysis of this effect in graphite. He concluded that this anomalous hump indicates a group of fast minority carriers that are dominant in the low field region where first order theory prevails.

Oscillations in the Hall potential appear in the work of Borovik<sup>23</sup> at very high fields. The high precision voltage determination employed in the measurements reported here allowed a more detailed observation of the oscillatory behavior of this effect. Measurements made at different orientations, but not reported here, are also in agreement with the extensive studies made by Borovik on the angular dependence of the effect and confirmed his findings that the  $\rho_{31}$  component of the tensor is an even function of the field.

### $\sigma$ Curves

The computed values of  $\sigma_{11}$  and  $\sigma_{21}$  plotted against  $1/H$  are shown in Fig. 11. The  $\sigma_{11}$  curve is almost purely monotonic except at the lower end of the  $1/H$

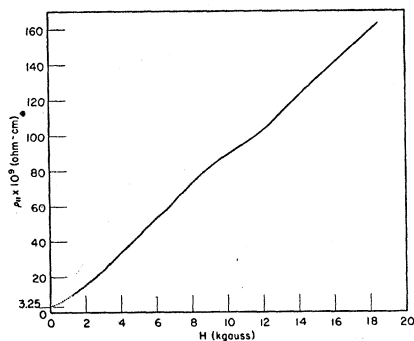


FIG. 10. The total magnetoresistance,  $\rho_{11}$ , versus the magnetic field,  $H$ .

<sup>44</sup> A. H. Wilson, *Theory of Metals* (Cambridge University Press, New York, 1953), 2nd ed.

axis, exhibiting only a negligible oscillatory component, while the  $\sigma_{21}$  curve shows pronounced oscillations. The unmodified Zil'berman theory predicts the opposite behavior (i.e., oscillations in  $\sigma_{11}$ , no oscillations in  $\sigma_{21}$ ). It is interesting to note that for low values of magnetic field, i.e.,  $1/H > 35 \times 10^{-5}$  gauss<sup>-1</sup>, the oscillations that are present in the  $\sigma_{21}$  curve are almost the pure fundamental of  $\tilde{\rho}_{21}$ . Then, in the intermediate field range ( $24$ – $35 \times 10^{-5}$  gauss<sup>-1</sup>) the second harmonic becomes detectable. Finally, for  $1/H < 24 \times 10^{-5}$  gauss<sup>-1</sup> the presence of the third harmonic is indicated by the flattening out of the "valleys" between the peaks of the fundamental. The average period of  $\sigma_{21}$  is  $6.14 \times 10^{-5}$  gauss<sup>-1</sup>, in very good agreement with  $\tilde{\rho}_{21}$ . Both of these curves are calculated from data taken at 1.2°K.

### Comparison of the Adiabatic and Isothermal Hall Effects

When the Hall potential is measured below 2.18°K, the superfluid helium keeps the crystal under isothermal

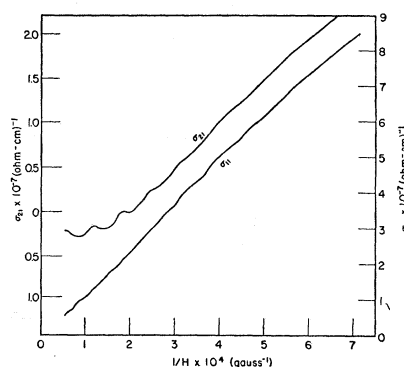


FIG. 11. The calculated values of the components of the conductivity tensor,  $\sigma_{ih}$ , versus the reciprocal of the magnetic field.

conditions. Above this temperature the helium I bath, despite the bubbling and convection currents, does not keep the crystal perfectly isothermal. In fact, large thermoelectric effects can be detected under such conditions.<sup>23</sup> The Hall effect measured above the  $\lambda$  point corresponds to a state between isothermal and adiabatic conditions. Therefore, qualitative indications of the different behavior of isothermal and adiabatic Hall potentials can be obtained by comparing data at 2.1°K and 2.2°K. From Jan<sup>29</sup> it is seen that the expected difference between the two effects is given by  $\epsilon_{11}\pi_{21}/\lambda_{11}$ , and from Fig. 6 it is possible to see that the difference of the curves  $\tilde{\rho}_{21}(2.2^\circ\text{K})$  and  $\tilde{\rho}_{21}(2.1^\circ\text{K})$  is primarily the second harmonic of the  $\tilde{\rho}_{21}$  oscillation. The interpretation of this is not certain since one might expect  $\pi_{21}$  to have the same fundamental as  $\tilde{\rho}_{21}$  and  $\epsilon_{21}$ , and  $\lambda_{11}^{-1}$  has been shown to be a relatively smooth valued function of the magnetic field.<sup>24</sup> However, if  $\epsilon_{11}$  also exhibits oscillations of the same fundamental period as  $\epsilon_{21}$ , then the product  $\pi_{21}\epsilon_{11}$  would have an



effective period of one-half the fundamental, i.e., the second harmonic.

**Comments on Zil'berman's Theory**

In assuming a quadratic dispersion law, Zil'berman's theory implicitly guarantees the constancy of  $(N_2 - N_1)$  as a function of magnetic field. However, in the case in which portions of the Fermi surface are open or are in sufficient proximity<sup>45</sup> to open constant energy surfaces the concepts of "number of holes" and "number of electrons" are not valid and should be replaced by an effective number of carriers which could be a fairly arbitrary function of the magnetic field. Also, by assuming that  $\beta H \ll E_0$  Zil'berman has placed himself in a position in which the constancy of the effective number of carriers of a closed region of the Fermi surface is assured. However, from an examination of our experimental results (e.g., Fig. 7), one can see that  $\beta H \sim E_0$  for  $H = 16$  kgauss.

The general physical interpretation of these oscillations is that for every complete period of the oscillations in the experimental quantity one of the quantized orbital energy levels of the carriers passes through the Fermi surface. Hence, this implies in the case of zinc that for  $H > 16$  kgauss there is, at most, one allowed energy level still within the Fermi surface. Therefore, if the magnetic field were allowed to increase indefinitely, the chemical potential,  $E_0$ , of this region of the Fermi surface must also increase without limit. This is a physically unacceptable conclusion.

A more feasible model is that of Blackman<sup>37</sup> and Levinger and Grimsal<sup>38</sup> in which the number of carriers in this region of the Fermi surface increases monotonically and then oscillates as the magnetic field is allowed to decrease from an infinite value. The monotonic increase corresponds to the approaching coincidence of the first orbital quantum level with the Fermi surface, and the subsequent oscillations correspond to the passage of higher levels through the Fermi surface.

A further correction to  $\sigma_{21}$  would be achieved if terms corresponding to the effects of elastic scattering caused by crystal defects were introduced. This could possibly be done by a similar procedure used by Zil'berman in calculating these terms for  $\sigma_{11}$ .

**Correlations**

If it is supposed that the oscillatory component of  $\sigma_{21}$  is much more significant than that of  $\sigma_{11}$ , some correlation can be found relating the sign reversal of  $\rho_{21}$ , Fig. 8, the phase reversal of  $\tilde{\rho}_{11}$ , and the presence of a large second harmonic in the neighborhood of the phase reversal. An explanation of the positive quadratic shape of the envelope to the  $\tilde{\rho}_{11}$  curve, Fig. 5, also follows. The calculated  $\sigma$  curves, Fig. 11, lend empirical

<sup>45</sup> F. J. Blatt, in *Solid-State Physics*, edited by F. Seitz and D. Turnbull (Academic Press, Inc., New York, 1957), Vol. IV, p. 226.

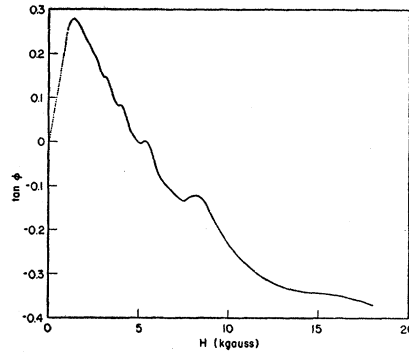


Fig. 12. The tangent of the Hall angle,  $E_2/E_1$ , versus the magnetic field,  $H$ .

support to this assumption. The quantity  $\sigma_{11}$ , which is directly related to Zil'berman's  $f$  function, exhibits an almost negligible oscillatory component, and  $\sigma_{21}$ , which is proportional to the effective number of carriers, has a definite oscillatory character.

We may write,

$$\rho_{11} = \frac{1}{\sigma_{11}(1 + \tan^2 \varphi)}$$

From Fig. 12 for the magnetic field range of this experiment,  $-0.3 \leq \tan \varphi \leq 0.3$ . Therefore, to a fairly good approximation,

$$\rho_{11} \cong (1/\sigma_{11})(1 - \tan^2 \varphi \dots)$$

Since  $\sigma_{11}$  is assumed to be a smooth function of the field, it can be seen from the above that

$$\tilde{\rho}_{11} \cong -\tan^2 \varphi / \sigma_{11}$$

A consideration of the field dependence of  $\tan \varphi$ , Fig. 12, shows that this relationship predicts the quadratic curvature of the envelope of  $\tilde{\rho}_{11}$  observed in Fig. 5. It also predicts the large second harmonic in the neighborhood of the phase inversion point of  $\tilde{\rho}_{11}$ .

In the magnetic field ranges where  $\tilde{\rho}_{21} \ll \rho_{21}$  ( $H < 3.5$  kgauss and  $H > 5$  kgauss) we may write  $\tilde{\rho}_{21} = \delta \rho_{21}$ . Similarly where  $\tilde{\rho}_{11} \ll \rho_{11}$  (this is true for all values of  $H$ )  $\tilde{\rho}_{11} = \delta \rho_{11}$ . Under similar restrictions, this same approximation can be made for  $\sigma_{11}$  and  $\sigma_{21}$ .

$$\delta \rho_{11} = [(\sigma_{21}^2 - \sigma_{11}^2) \delta \sigma_{11} = 2\sigma_{11}\sigma_{21} \delta \sigma_{21}] / (\sigma_{21}^2 + \sigma_{11}^2)^2$$

Since  $\tilde{\sigma}_{11} = \delta \sigma_{11}$  is assumed to be negligible,

$$\delta \rho_{11} \cong -2\sigma_{11}\sigma_{21} \delta \sigma_{21} / (\sigma_{11}^2 + \sigma_{21}^2)^2 \cong -2\sigma_{11}\rho_{21} \tilde{\rho}_{21}$$

For  $H < 4$  kgauss  $\rho_{21} > 0$  and for  $H > 5$  kgauss  $\rho_{21} < 0$  (see Fig. 8). Therefore,  $\tilde{\rho}_{11}$  is  $\pi$  out of phase with  $\tilde{\rho}_{21}$  for low fields and then reverses its phase at  $H = 4.5$  kgauss and is in phase with  $\tilde{\rho}_{21}$  at higher fields.

From the experimental results for the thermal potentials empirical relationships can also be developed between the longitudinal and the transverse effects. Alers<sup>24</sup> measured  $\lambda_{11}^{-1}$  along with  $\rho_{11}$  and found that

both exhibited a magnetic field dependence of the same form reported here in  $\rho_{11}$ , i.e., a very small oscillatory component superimposed on a large monotonic component. This implies that the amplitudes of  $\epsilon_{11}'$  and  $\epsilon_{21}'$ , as given in Eq. (4), have a varying scale proportional to  $\lambda_{11}^{-1}$ , which to a first approximation is linear. This introduces no change in the period of  $\epsilon_{11}'$  and  $\epsilon_{21}'$ .

With reference to Eq. (4), if  $[\epsilon_{11} - (1/e)\partial E_0/\partial T]$  is considered to be negligible, we may write

$$\epsilon_{11}' = \epsilon_{21}' \tan \varphi.$$

This predicts the phase inversion of  $\epsilon_{11}'$  at 4.5 kgauss shown in Fig. 4, and the predominant second harmonic in this region, Fig. 9, since the oscillations in  $\tan \varphi^{46}$  are in phase with  $\epsilon_{21}'$  in the neighborhood of the phase inversion point. The Zil'berman theory which fails to predict oscillations in  $\sigma_{21}$  disagrees also with the experimental results on the thermoelectric power. Neglecting the Etingshausen-Nernst coefficient  $\epsilon_{21}$ , Eq. (12) derived from his theory most obviously does not agree with the experimental results, which more closely fit the relation  $\epsilon_{11}' = \epsilon_{21} \tan \varphi$ .

The absolute thermoelectric power is linear in  $e$ , i.e., if conduction is caused by electrons, it is negative, or if caused by "holes," it is positive.<sup>46</sup> Therefore, the absence of a monotonic term in  $\epsilon_{11}'$  makes the above assumption reasonable. It would be extremely fortuitous if the magnetic field dependence of  $\epsilon_{11}$  and  $\partial E_0/\partial T$  were of the same form and magnitude such as to effectively cancel each other's contribution to the measured potentials. It would seem that it is more reasonable to assume they are individually negligible.

#### Temperature and Field Dependence of the Amplitude

In the liquid helium temperature range, the amplitudes of the oscillations of all four effects were almost independent of the temperature. This can be seen for  $\bar{\rho}_{21}$  in Fig. 6. Probably more information about the

temperature dependence of the amplitude could be had if these experiments were repeated at liquid hydrogen temperatures. Possibly a dependence of the period on temperature might be detected in this range, which could be correlated with the results of Berlincourt and Steele in their study of the magnetization.<sup>22</sup>

The field dependence of the amplitude of the various oscillations could not be fitted to any theoretical expressions known to the authors for any of these effects.

#### VII. CONCLUSIONS

The constant energy surfaces in zinc are very complex, and a complete description of their topology will require more detailed and intensive experimentation than is reported in this paper. A study of these galvanomagnetic and thermomagnetic phenomena at much higher fields might reveal oscillations which would give detailed information about relatively large regions of the Fermi surface. Also, according to Lifshitz and Peschanskii<sup>47</sup> the asymptotic behavior of the conductivity tensor  $\sigma_{ik}$  in strong magnetic fields for open Fermi surfaces can differ essentially from its asymptotic behavior when the constant energy surfaces are closed. Therefore, an angular study of the galvanomagnetic effects in large magnetic fields would reveal when the carrier trajectories lie along open or closed paths.

Preparations are being made to measure the thermal magnetoresistance and the Peltier tensors in the same zinc crystal used in this present study. It will then be possible to extract  $\epsilon_{11}$  and  $\epsilon_{21}$  from the thermomagnetic potentials presented in this paper and to determine the validity of the Wiedemann-Franz ratio for these oscillatory effects.

A much more fundamental feature is that the combined data of this present paper and the proposed experiments will enable one to test the applicability of Onsager's reciprocal relations<sup>29</sup> to these oscillatory effects.

<sup>46</sup>  $\tan \varphi$  is the experimentally determined Hall angle, Fig. 12, which by virtue of assumption of the validity of the Wiedemann-Franz ratio is identical to the Righi-Leduc angle.

<sup>47</sup> I. M. Lifshitz and V. G. Peschanskii, J. Exptl. Theoret. Phys. (U.S.S.R.) **35**, 1251 (1958) [translation: Soviet Phys.—JETP **8**, 875 (1959)].